catalysts

MDPI

Article

Silver Dependent Enantiodivergent Gold(I) Catalysed Asymmetric Intramolecular Hydroamination of Alkenes: A Theoretical Study

Ruchi Dixit [1,2], Himanshu Sharma [1,2], Francine Agbossou-Niedercorn [3], Kumar Vanka [1,*] and Christophe Michon [4,*]

[1] CSIR-National Chemical Laboratory, Physical and Material Chemistry Division, Dr. Homi Bhabha Road, Pashan, Pune 411008, India
[2] Academy of Scientific and Innovative Research (AcSIR), Ghaziabad 201002, India
[3] Centrale Lille, Université de Lille, CNRS, UMR 8181, UCCS, Unité de Catalyse et Chimie du Solide, Avenue Mendeleiev, CEDEX, 59655 Villeneuve d'Ascq, France
[4] Ecole Européenne de Chimie, Polymères et Matériaux, Université de Strasbourg, CNRS, LIMA, UMR 7042, 25 Rue Becquerel, 67087 Strasbourg, France
* Correspondence: k.vanka@ncl.res.in (K.V.); cmichon@unistra.fr (C.M.)

Abstract: We report a theoretical study of the first silver-dependent enantiodivergent gold-catalysed reaction. The combination of a single chiral binuclear gold(I) chloride complex and silver perchlorate catalyses the asymmetric intramolecular hydroamination of alkenes and affords both enantiomers of the products by applying a simple solvent change from toluene to methanol. A gold-silver chloride adduct that occurs only in methanol appears to control the enantioinversion. If one gold atom coordinates and activates the alkene moiety, the other gold is included in an adduct with silver chloride, which coordinates a methanol solvent molecule and further interacts with the amine function. If the use of toluene implies free anions and affords (*S*)-enantiomer, methanol allows a proximal interaction with the amine, leads to an opposite stereodifferentiation of the two diastereomeric intermediates during the final protodeauration step and results in the (*R*)-enantiomer.

Keywords: alkene; enantiodivergent catalysis; gold; hydroamination; silver

Citation: Dixit, R.; Sharma, H.; Agbossou-Niedercorn, F.; Vanka, K.; Michon, C. Silver Dependent Enantiodivergent Gold(I) Catalysed Asymmetric Intramolecular Hydroamination of Alkenes: A Theoretical Study. *Catalysts* **2022**, *12*, 1392. https://doi.org/10.3390/catal12111392

Academic Editors: Cyril Nicolas and Isabelle Gillaizeau

Received: 18 October 2022
Accepted: 6 November 2022
Published: 8 November 2022

1. Introduction

The shortest synthetic route to secondary and tertiary amines is the hydroamination of unactivated alkenes [1–4]. Regarding the enantioselective synthesis of amines, metal catalysis is the most studied and privileged hydroamination route [1]. Throughout the past decade, intra- and intermolecular hydroamination reactions of various C-C multiple bond substrates such as alkynes, alkenes, allenes, and dienes have been successfully performed using gold catalysts [5–8]. However, the gold-catalysed hydroamination of alkenes has been less studied in its asymmetric version as high temperatures, long reaction times, and strict conditions are generally required [3,5–8]. To the best of our knowledge, seven publications have addressed this topic to date [9–16]. First, intermolecular hydroaminations of ethylene and 1-alkenes with cyclic ureas were performed in high yields and enantioselectivities using binuclear gold(I) catalysts based on 2,2′-bis(diphenylphosphino)-1,1′-biphenyl (BIPHEP) ligands [9]. Later, intramolecular hydroaminations of N-alkenyl ureas were effectively catalysed at room temperature with good yields and average enantioselectivities through the use of tropos BIPHEP-binuclear gold(I) species combined with chiral anions [10]. Thereafter, intramolecular hydroamination of N-alkenyl tosylates was obtained in moderate yields and enantioselectivities at high temperatures and reaction times while using several mononuclear gold(I) complexes based on axially chiral ligands [11]. In 2014, Widenhoefer et al. reported on the combination of a mono- or binuclear gold complex with AgOTf (5 mol%) in methanol to catalyse the intramolecular hydroamination of N-4-pentenylcarbamates and

ureas [12]. Average to high yields and enantioselectivities were obtained at room temperature, 0 °C or −20 °C within 2 or 3 days of reaction when a binuclear gold(I)-(*S*)-DTBM-MeO-BIPHEP catalyst was used. In addition, active mononuclear gold catalysts based on monodentate phosphines with a 2-(diphenylphosphino)-2′-methoxy-1,1′-binaphthyl (MOP) ligand skeleton led to quantitative reactions with low enantioselectivities [12]. Following our ongoing interest in hydroamination reactions [17–20], we reported the intramolecular hydroamination of several alkenes at mild temperatures in good yields and average enantioselectivities using catalysts based on mononuclear gold(I)-phosphoramidite complexes [13]. Several binuclear gold(I)-diphosphine catalysts were subsequently studied and we showed the combination of a binuclear gold(I) chloride species built on a specific 5,5′-bis(diphenylphosphino)-4,4′-bi-1,3-benzodioxole (SEGPHOS) diphosphine ligand with a selected silver salt effectively catalysed the intramolecular hydroamination of alkenes at mild temperatures in high yields and enantioselectivities [14–16]. Surprisingly, the use of the same chiral gold catalyst allowed the synthesis of both enantiomers of the products by changing the solvent from toluene to methanol (Scheme 1).

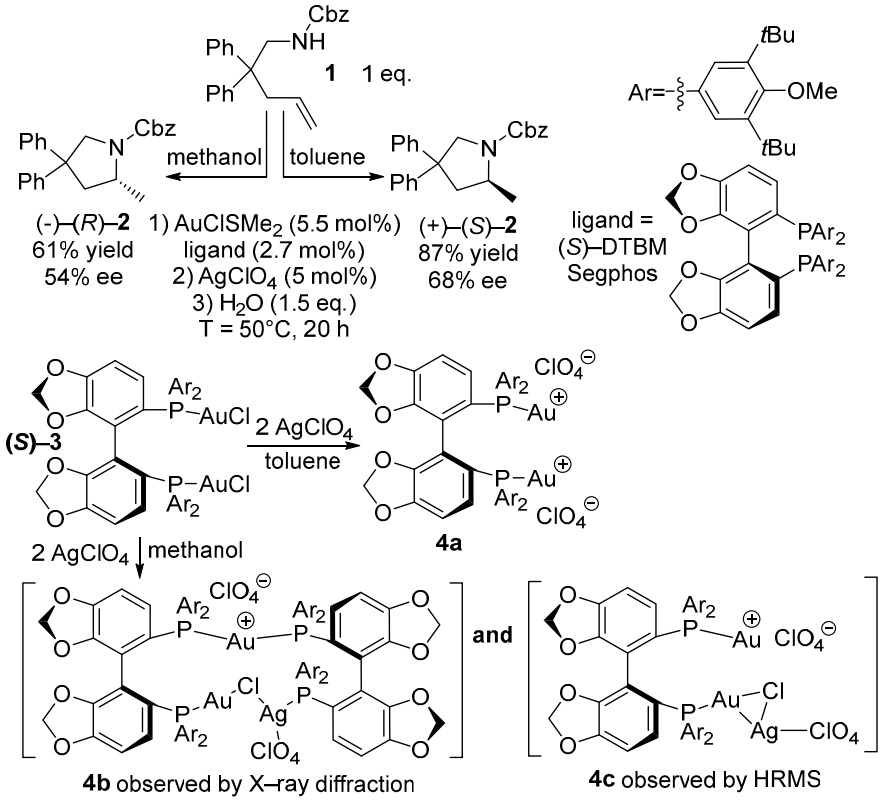

Scheme 1. Enantiodivergent intramolecular hydroamination of alkenes catalysed by gold(I) cationic complex and preparation of gold(I) cationic complexes **4a**, **4b** and **4c**.

Various enantiodivergent reactions have been reported using a single chiral catalyst [21–24] and their mechanisms remain often not well understood. In some cases, kinetic analyses and calculations demonstrated that an enthalpy-entropy compensation often controlled solvent-dependent stereodiscrimination [25–27]. Concerning gold enantiodivergent catalysis, the enantioinversion was shown to be induced by parameters such as solvent, temperature or counterion, alone or in combination with one another [28–33]. By comparison, our enantiodivergent reaction [16] proved to be strictly independent of the reaction temperature or of the nature of the catalyst anion and the ion pairing [34,35]. It displayed similar first-order kinetic rate law with respect to substrate concentration in both solvents. In addition, any Brønsted acid catalysis [36] was unlikely and we confirmed the gold active species' nuclearity remained unchanged during the entire catalytic reaction [37–41] and there was no in situ kinetic resolution involved [42]. Finally, even though the contri-

bution of anion and cation π-interactions was shown critical in gold catalysis [11,43–46], our results ruled out any interactions [43–49] between the catalyst and toluene along the enantiodivergent reaction.

Similar to many organometallic pre-catalysts, a huge number of gold neutral complexes require activation by halide abstraction through the use of silver salts and several reports highlighted the positive or negative impacts of silver on yields and selectivities [50–59]. Gold-catalysed intramolecular hydroarylation of allenes and hydroalkoxylation of alkynes were affected by off-cycle species between silver and active gold intermediates, which reduced the concentration and catalytic activity of in-cycle gold species [50,56]. Moreover, gold-catalysed intramolecular hydroamination of alkynes was shown to switch from 5-exo-dig to 6-endo-dig regioselectivity through the use of a silver additive, which was also an active catalyst leading exclusively to the six-membered ring product [58]. In addition, gold and silver species proved to be effective and synergistic in cooperative catalysis for reactions such as the alkynylation of cyclopropenes, the dehydrogenative cross-coupling reaction between pyrazoles and fluoroarenes, olefin cyclopropanation, 1,5-enyne isomerisation into bicyclo [3.1.0] hexanes and cyclopentene or cyclopentenone synthesis [60]. Whether silver and chloride bind cationic monomeric and oligomeric phosphine gold chloride complexes through several bonding modes [61–65], the implication of such gold-silver chloride species in catalysis has never been rationalised.

The characterisation at the solid state of a dicationic gold complex similar to **4a** but with two tetrafluoroborate anions was previously reported by us (Scheme 1) [15]. Furthermore, we noticed crystals obtained in methanol-diethyl ether mixtures revealed complex **4b** comprising two (*S*)-DTBM-Segphos ligands coordinated to the two gold atoms in a trans-fashion with an additional silver chloride molecule inserted into one of the phosphorous-gold bonds (Scheme 1) [16]. Whereas a gold(I) NHC complex was once shown to form a triangular fragment with silver chloride [65], species **4b** illustrated a new and rather linear adduct, gold and silver being coordinated to two distinct phosphorous atoms and connected through a μ-chloro bridge. Taking into account that some silver chloride adducts were previously characterised for gold(I) [6,65] and mass spectrometry had already allowed the identification of several gold intermediates [66–68], we analysed our samples by ESI-FT mass spectrometry in methanol and clearly identified the binuclear monocationic gold complex **4c** with a triangular silver-chloride adduct [65]. Interestingly, this complex was not observed in toluene by CSI-MS and by using a mass spectrometer coupled with an additional liquid injection field desorption ionisation (LIFDI) source [69,70]. Though we remained careful about drawing a parallel between characterisations obtained by X-ray diffraction and mass analyses and results obtained in a solution phase synthesis or catalysis, we started a theoretical study on this first silver and solvent-dependent enantiodivergent gold catalysed reaction.

2. Results

We started our study focusing on the reaction mechanism in toluene using catalyst **4a**. The low polarity of the solvent results in the absence of any gold-silver chloride adduct (Figure 1) [16]. The first step implies an electrophilic activation of the alkene by the gold catalyst to lead to intermediate **1** with ΔE and ΔG of, respectively, −18.8 and −1.3 kcal/mol (Figure 1, Table S1). In the second step, the amine undergoes a reversible nucleophilic attack [71–78], which preferentially forms the intermediate **2a** of the (*R*) configuration with ΔE and ΔG of, respectively, −19.8 and 2.5 kcal/mol over intermediate **2b**, whose ΔE and ΔG values are, respectively, −15.5 and 6.9 kcal/mol. In the third step, the tautomerisation of the resulting carbamates proceeds through the possible assistance of the perchlorate anion [79–85] to lead to intermediate **3a** with ΔE and ΔG of, respectively, −18.1 and 4.1 kcal/mol and intermediate **3b** with ΔE and ΔG of, respectively, −15.3 and 6.3 kcal/mol. Finally, the protodeauration [71–75] proceeds through a proton transfer assisted by the perchlorate anion [79–85], which defines the stereochemical outcome of the hydroamination

by privileging the formation of the cyclised amine product (*S*)-**2** with ΔE and ΔG of, respectively, −24.2 and −20.8 kcal/mol as shown in Figure 1.

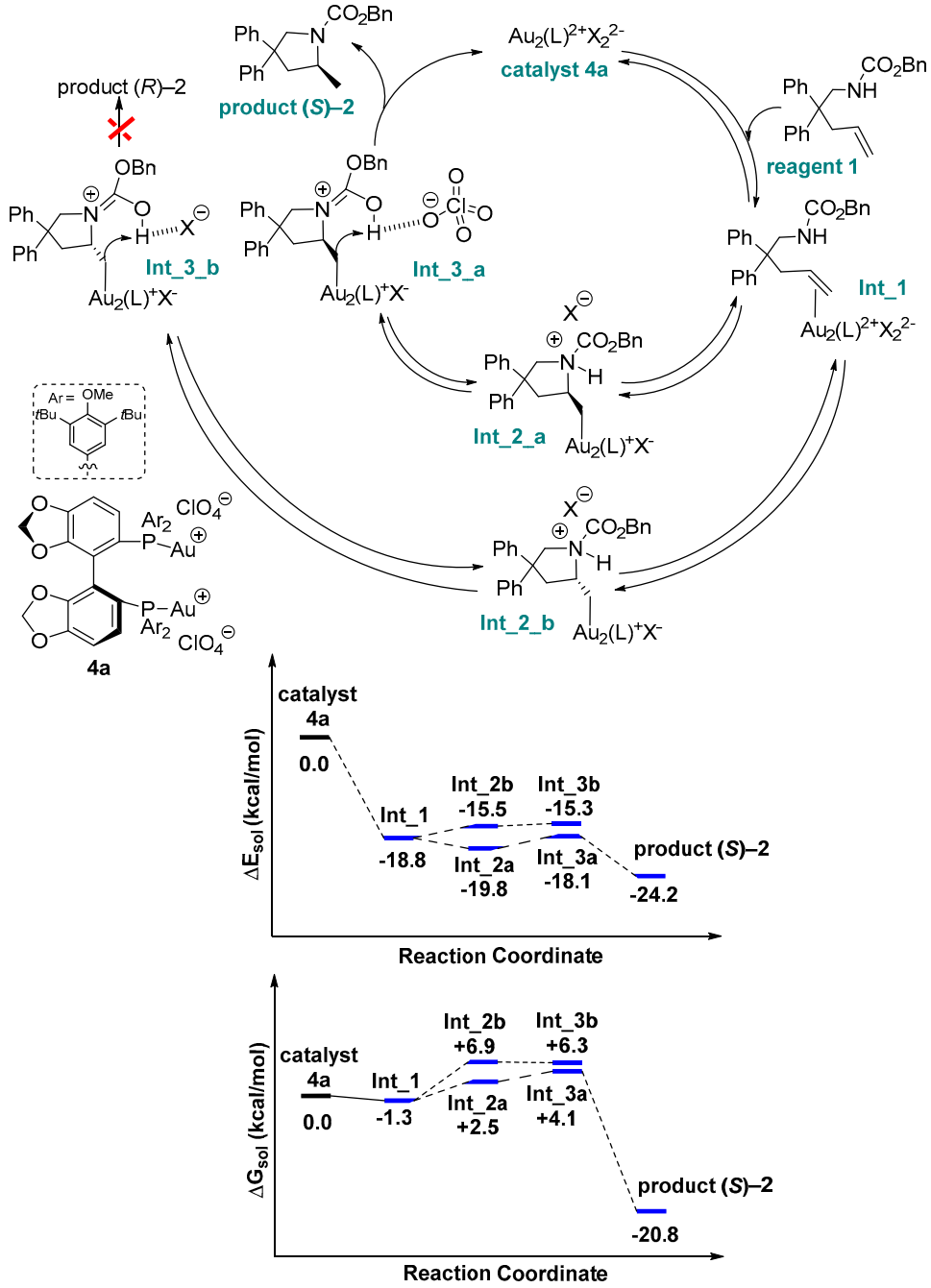

Figure 1. The proposed reaction mechanism for the formation of the amine product (*S*)-**2** in toluene using catalyst **4a**. The electronic energy profile is shown at PBE0/def2-TZVP//PBE/def-TZVP level of theory. All values are in kcal/mol.

The reaction mechanism in methanol was then considered, the high polarity solvent allowing the presence of a gold-silver chloride adduct [16]. By comparison to catalyst **4c**, the use of catalyst **4b** proved to be not favourable for computational studies due to prohibitively high computational costs. Hence, the mechanistic studies were completed with catalyst **4c** (Figure 2, Table S2).

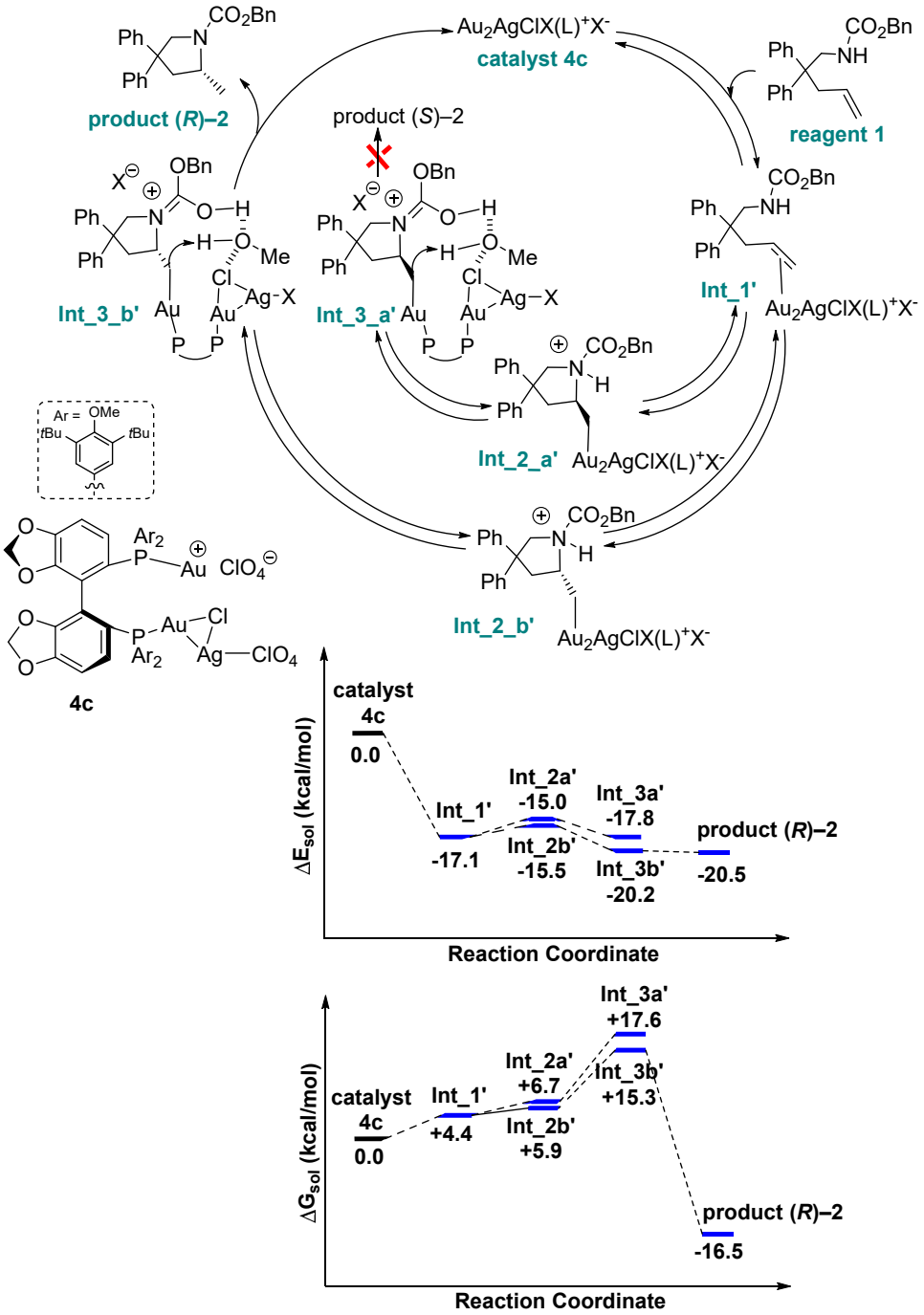

Figure 2. The proposed reaction mechanism for the formation of the amine product (*R*)-**2** in methanol using catalyst **4c**; calculations at the PBE0/def2-TZVP//PBE/def-TZVP level of theory with DFT. All values are in kcal/mol.

In the first step, the electrophilic activation of the alkene by the gold catalyst led to intermediate **1**′ with ΔE and ΔG of, respectively, −17.1 and 4.4 kcal/mol. In the second step, the reversible nucleophilic attack of the amine [71–79] formed preferentially intermediate **2b**′ of (*S*) configuration with ΔE and ΔG of, respectively, −15.5 and 5.9 kcal/mol over intermediate **2a**′ whose ΔE and ΔG were of, respectively, −15.0 and 6.7 kcal/mol (Figure 2). In the third step, the resulting carbamates underwent a tautomerisation through the possible assistance of the methanol, the perchlorate anion being far away from the cationic organic moiety due to the poor ion pairing induced by the strong polarity of the methanol [79–85]. This preferentially leads to intermediate **3b**′ with ΔE and ΔG of, respec-

tively, −20.2 and 15.3 kcal/mol over intermediate **3a′** with ΔE and ΔG of, respectively, −17.8 and 17.6 kcal/mol. In the last step, the final protodeauration defined the stereochemical outcome of the hydroamination by privileging the formation of the cyclised amine (*R*)-**2** with ΔE and ΔG of, respectively, −20.5 and −16.5 kcal/mol as shown in Figure 2.

This step may proceed through a proton transfer assisted by a methanol molecule [86,87] which was no longer free but coordinated to the gold-silver chloride adduct as highlighted by intermediate **3b′** displayed in Figure 3. The distance between the silver and the oxygen atoms was 2.83 Å and NCI analysis confirmed their interaction (Figures S1–S4). It was worth noting the electron-poor chloride and the oxygen atom of the methanol molecule were too far (3.539 Å) to allow any interaction such as a halogen bond [88–90] as confirmed by the NCI plot. Furthermore, this coordinated methanol molecule was involved in two proximal interactions allowing the final protodeauration step, first through its oxygen and the proton of the carbamate tautomer (1.42 Å) and second, through its hydrogen and the carbon connected to the second gold atom (2.40 Å) (Figure 3).

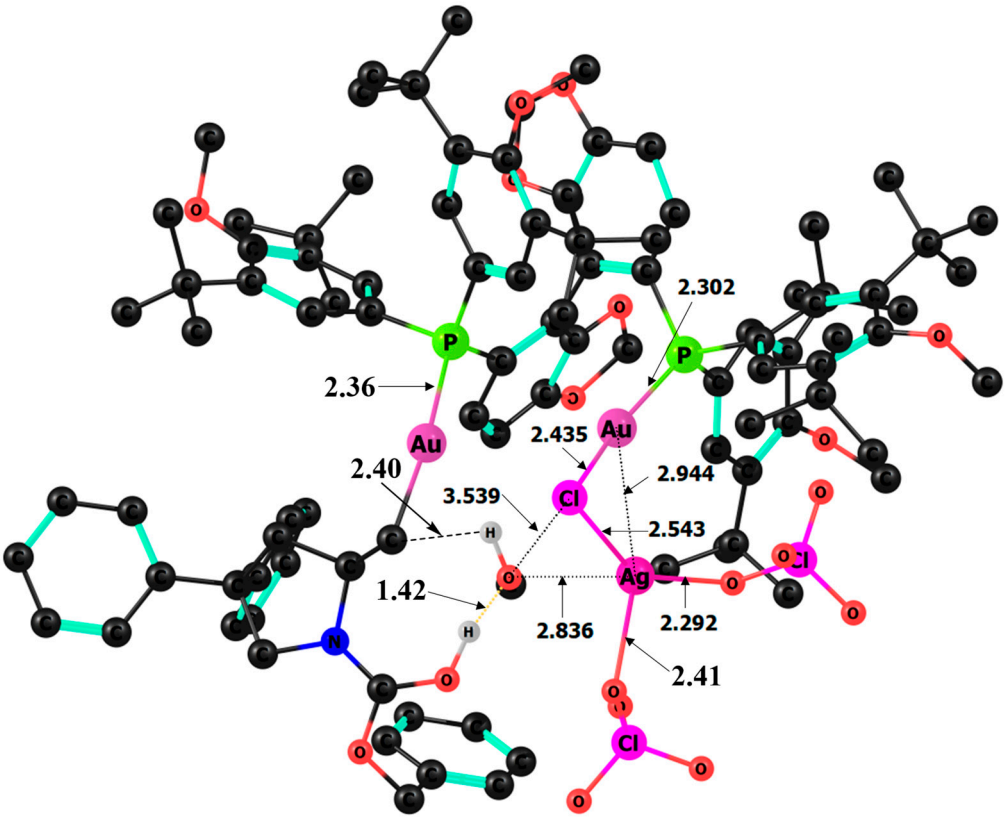

Figure 3. The optimised geometry of intermediate **3_b′** implied in the reaction mechanism in methanol using catalyst **4c** and one molecule of solvent methanol. All the hydrogen atoms attached to carbon atoms are omitted for the purpose of clarity. Intermediate **3_b′** implied in the reaction mechanism in methanol using catalyst **4c** and one molecule of solvent methanol.

We also investigated another possibility (Figure 4, Table S3), where intermediate **3a′** and **3b′** would be formed without the assistance of a molecule of methanol (Figure 4). The electronic and Gibbs free energy for the formation of intermediate **3a′** were, respectively, −15.3 and 8.1 kcal/mol and, by comparison to the formation of intermediate **3b′** they were, respectively, −9.1 and 11.6 kcal/mol. The calculations suggested that the formation of intermediate **3a′** was thermodynamically favourable over intermediate **3b′**, which led to amine product (*S*)-**2** and therefore did not match with the experimental outcome of this catalytic hydroamination.

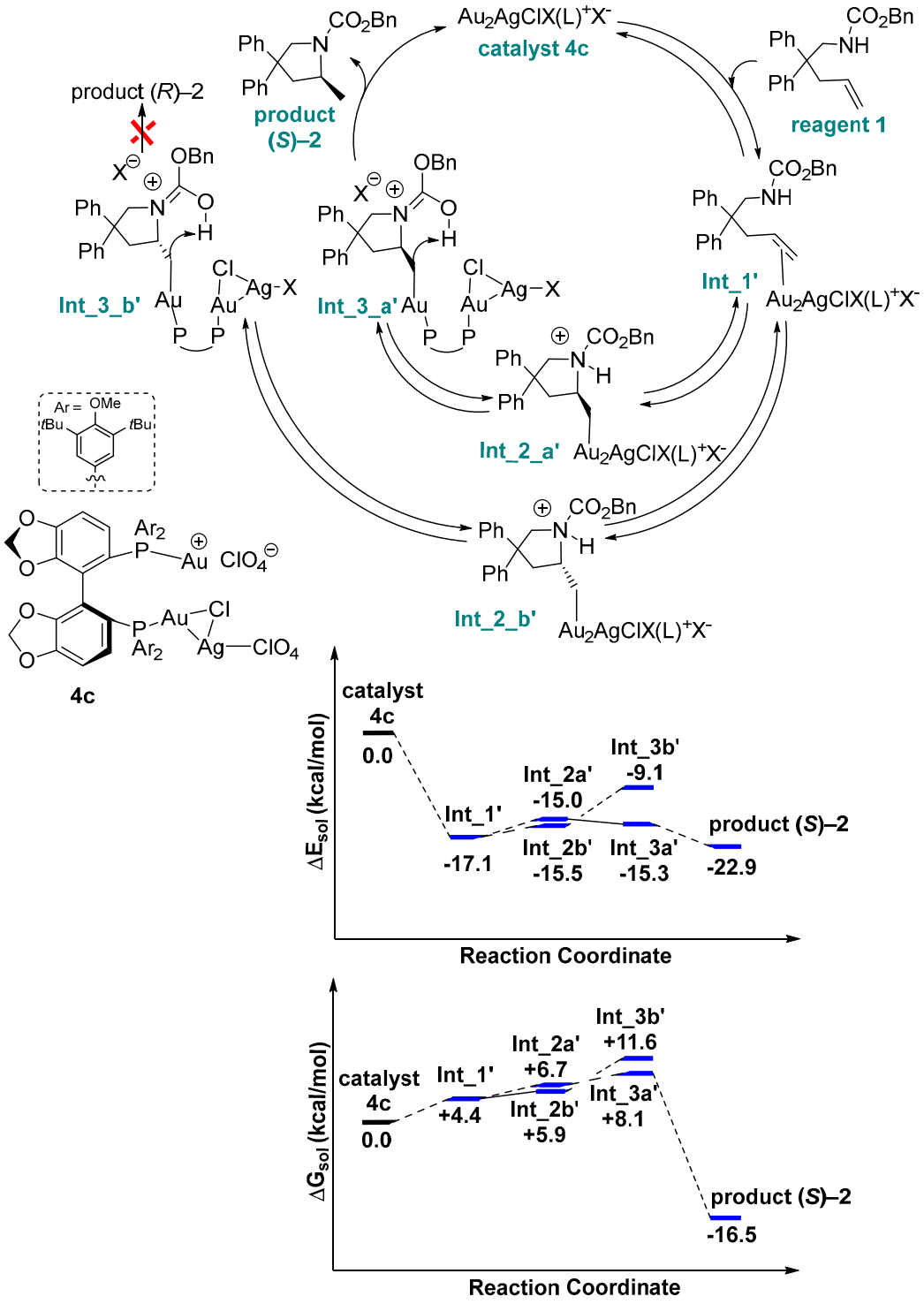

Figure 4. The proposed reaction mechanism for the formation of the amine product (*S*)-**2** in methanol using catalyst **4c**, and without the assistance of one methanol molecule. The electronic energy profile is shown at PBE0/def2-TZVP//PBE/def-TZVP level of theory. All values are in kcal/mol.

Hence, the enantioinversion observed by switching from toluene to methanol could be explained by the gold-silver chloride adduct that formed only in methanol. While one gold atom of the catalyst activates the alkene function, the second gold atom of the catalyst coordinates silver chloride to form an adduct which interacts with a methanol molecule. The resulting intermediate allowed proximal interactions with the carbamate function and the alkene moiety. By comparison with toluene which affords (*S*)-enantiomer of cyclised

amine **2**, these proximal interactions allow an opposite stereodifferentiation of the two diastereomeric intermediates by setting the CH_2-Au group on another face of the medium plane defined by the N-heterocycle and by considering the steric hindrance of the catalytic intermediate. As a result, the final protodeauration step in methanol leads to the observed opposite (*R*)-enantiomer of cyclised amine **2** through the assistance of a methanol molecule, the latter being no longer free but coordinated to a gold-silver chloride adduct.

3. Material and Methods

3.1. General Procedure for the Catalysis

Safety concern. Caution! Perchloric acid as well as all organic and organometallic perchlorate salts are often explosive and are thus highly dangerous [91].

In a glovebox, $AuS(Me)_2Cl$ (0.01 mmol, 2.95 mg) and (*S*)-DTBM-Segphos (0.005 mmol, 5.90 mg) are disposed of in a first Schlenk flask. Under a nitrogen atmosphere, dry dichloromethane (1 mL) is then added, and the resulting mixture is stirred for 1 h at room temperature. Afterwards, the solvent is evaporated under vacuum and the resulting solid is dried 30 min before addition of $AgClO_4$ (0.009 mmol, 1.87 mg) in a glovebox. Under a nitrogen atmosphere, dry toluene or methanol (1 mL) is added and the resulting solution is stirred for 30 min before being transferred to a second Schlenk flask containing the corresponding substrate (0.18 mmol). Finally, H_2O (0.28 mmol, 5 µL) is added under nitrogen to the reaction mixture. After 20 h under stirring at 50 °C, the solution is filtered through a pad of silica gel using dichloromethane as solvent. After evaporation of solvents under vacuum, the resulting oil is analysed by ^{1}H NMR and HPLC using Daicel Chiralpak^{TM} IA chiral stationary phase (at 25 °C) with (90/10) *n*-hexane/*i*PrOH, 1.0 mL/min, λ = 200 nm (Figures S5–S7) [16].

3.2. Computational Details

All the geometrical optimisation in this study was performed with density functional theory (DFT), with the aid of the Turbomole 7.1 suite of programs [92], using the PBE functional [93] and the def-TZVP [94] basis set. The single-point calculations were carried out at PBE0/def2TZVP level of theory [95–97]. The resolution of identity (RI) [98], along with the multipole accelerated resolution of identity (marij) [99] approximations were employed for an accurate and effective treatment of the electronic Coulomb term in the DFT calculations. Solvent corrections were incorporated with optimisation calculations using the COSMO model [100], with toluene (ε = 2.38) or methanol (ε = 32.7) as the solvents. We used Grimme's dispersion correction (DFT-D3) [101] to consider the long-range interactions. The values reported are ΔG values, with zero-point energy corrections, internal energy, and entropic contributions included through harmonic frequency calculations on the optimised minima, with the temperature set to 298.15 K. Harmonic frequency calculations were performed for all stationary points to confirm them as local minima. The NCIPLOT was employed as a computational index for studying weak noncovalent interactions using Multiwfn 3.8 software [102] and VMD for visualisation [103].

In the past years, multiple studies have been conducted on transition metal catalysts and their catalytic properties have been explored including theoretical studies. Functional PBE has been frequently employed [104,105], as it provides acceptable results for transition metal complexes. Moreover, the high-quality def-TZVP basis set that we have employed in the present work has previously been used to study several systems [106]. Furthermore, though it is always desirable to further increase predictive accuracy of computational studies, it consistently results in increased computational cost. Though the use of a hybrid functional such as PBE0 is a possible approach to achieve more accurate theoretical results, it tends to be more computationally expensive. By comparison, the PBE0 hybrid functional is made by mixing the Perdew-Burke-Ernzerhof (PBE) exchange energy and the Hartree-Fock exchange energy in a 3:1 ratio, along with the PBE correlation energy. In order to save some computational cost and still improve the results' accuracy, the structures optimised at

the PBE/def-TZVP level of theory have been studied further using single-point calculations at the PBE0/def2-TZVP level of theory.

4. Conclusions

To summarise, a binuclear gold(I) chloride complex based on DTBM-Segphos ligand was combined with silver perchlorate to catalyse effectively the asymmetric intramolecular hydroamination of alkenes with high yields and enantioselectivities, at mild temperatures and in presence of water. The use of such a single chiral binuclear gold catalyst led to both enantiomers of the products through a simple switch from toluene to methanol. The latter, a high polarity solvent, resulted in the formation of a gold-silver chloride adduct which interacted in a dual fashion with the N-alkenyl carbamate substrate. Indeed, according to our calculations, a gold atom of the catalyst bounds to the alkene function and the second gold atom coordinates silver chloride to form an adduct which interacts with a methanol molecule. The resulting intermediate allows proximal interactions with the carbamate function and the alkene moiety. Hence, by comparison with toluene, which involves free perchlorate anions to help the final protodeauration step, methanol itself coordinates with the catalyst, interacts with the aminoalkene to assist the proton transfer and allows the formation of the opposite enantiomer.

This work underlines the importance of the final protodeauration step in gold-catalysed reactions: it requires the assistance of an anion or a solvent to transfer the proton from the nucleophile reagent or other proton source to the carbon-gold bond and, finally defines the stereochemical outcome of the reaction. Therefore, interesting perspectives are offered for asymmetric organic reactions catalysed by chiral binuclear gold catalysts in combination with silver salts with the possibility to prepare from appropriately designed organic substrates both product enantiomers from a single chiral source through a change from an apolar to a polar solvent.

Supplementary Materials: The following materials are available online at https://www.mdpi.com/article/10.3390/catal12111392/s1, Figures S1–S4: NCI plot for non-covalent interaction between oxygen (of methanol) and Ag metal unit of **int_3b′**; Figures S5–S7: HPLC chromatograms; Tables S1–S3: electronic and Gibb's free energy for each chemical step of the studied catalytic cycles; x, y, z coordinates for the catalytic cycles in toluene and in methanol.

Author Contributions: Computational work and data collection, R.D. and H.S.; supervision, F.A.-N.; supervision, writing and editing, K.V. and C.M. All authors have read and agreed to the published version of the manuscript.

Funding: This research was sponsored by the Agence Nationale de la Recherche, grant number ANR-09-BLAN-0032-02. The CNRS, the Chevreul Institute (FR 2638), the Ministère de l'Enseignement Supérieur et de la Recherche, the Région Hauts-de-France and the FEDER are acknowledged for supporting and funding partially this work. This research has been performed as part of the Indian-French International Associated Laboratory for "Catalysis for Sustainable and Environmental Chemistry" (LIA CNRS MATSUCAT 2017–2021) and with the support of a CNRS International Emerging Action (IEA 2021).

Data Availability Statement: Data is contained within the article or Supplementary Material.

Acknowledgments: CM gratefully acknowledges the CNRS and the University of Strasbourg for their support.

Conflicts of Interest: The authors declare no conflict of interest.

References

1. Reznichenko, A.L.; Nawara-Hultzsch, A.J.; Hultzsch, K.C. Asymmetric hydroamination. *Top. Curr. Chem.* **2014**, *343*, 191–260. [CrossRef] [PubMed]
2. Huang, L.; Arndt, M.; Gooßen, K.; Heydt, H.; Gooßen, L.J. Late transition metal-catalyzed hydroamination and hydroamidation. *Chem. Rev.* **2015**, *115*, 2596–2697. [CrossRef] [PubMed]

3. Michon, C.; Abadie, M.-A.; Medina, F.; Agbossou-Niedercorn, F. Recent metal-catalysed asymmetric hydroaminations of alkenes. *J. Organomet. Chem.* **2017**, *847*, 13–37. [CrossRef]
4. Colonna, P.; Bezzenine, S.; Gil, R.; Hannedouche, J. Alkene Hydroamination via Earth-Abundant Transition Metal (Iron, Cobalt, Copper and Zinc) Catalysis: A Mechanistic Overview. *Adv. Synth. Catal.* **2020**, *362*, 1550–1563. [CrossRef]
5. Praveen, C. Carbophilic activation of π-systems via gold coordination: Towards regioselective access of intermolecular addition products. *Coord. Chem. Rev.* **2019**, *392*, 1–34. [CrossRef]
6. Lu, Z.; Hammond, G.B.; Xu, B. Improving Homogeneous Cationic Gold Catalysis through a Mechanism-Based Approach. *Acc. Chem. Res.* **2019**, *52*, 1275–1288. [CrossRef]
7. Campeau, D.; Leon Rayo, D.F.; Mansour, A.; Muratov, K.; Gagosz, F. Gold-Catalyzed Reactions of Specially Activated Alkynes, Allenes, and Alkenes. *Chem. Rev.* **2021**, *121*, 8756–8867. [CrossRef]
8. Zuccarello, G.; Escofet, I.; Caniparoli, U.; Echavarren, A.M. New-Generation Ligand Design for the Gold-Catalyzed Asymmetric Activation of Alkynes. *ChemPlusChem* **2021**, *86*, 1283–1296. [CrossRef]
9. Zhang, Z.; Lee, S.D.; Widenhoefer, R.A. Intermolecular Hydroamination of Ethylene and 1-Alkenes with Cyclic Ureas Catalyzed by Achiral and Chiral Gold(I) Complexes. *J. Am. Chem. Soc.* **2009**, *131*, 5372–5373. [CrossRef]
10. Kojima, M.; Mikami, K. Enantioselective Intramolecular Hydroamination of N-Alkenyl Ureas Catalyzed by tropos BIPHEP-Gold(I) Complexes with Au-Au Interaction. *Synlett* **2012**, *23*, 57–61. [CrossRef]
11. Sun, Y.W.; Xu, Q.; Shi, M. Synthesis of axially chiral gold complexes and their applications in asymmetric catalyses. *Beilstein J. Org. Chem.* **2013**, *9*, 2224–2232. [CrossRef] [PubMed]
12. Lee, S.D.; Timmerman, J.C.; Widenhoefer, R.A. Enantioselective Intramolecular Hydroamination of Unactivated Alkenes Catalyzed by Mono- and Bis(gold) Phosphine Complexes. *Adv. Synth. Catal.* **2014**, *356*, 3187–3192. [CrossRef]
13. Michon, C.; Abadie, M.-A.; Medina, F.; Agbossou-Niedercorn, F. Mononuclear gold catalysts for the asymmetric intramolecular hydroamination of alkenes. *Catal. Today* **2014**, *235*, 2–13. [CrossRef]
14. Abadie, M.-A.; Medina, F.; Agbossou-Niedercorn, F.; Michon, C. Efficient gold(I) catalysed asymmetric hydroamination of alkenes. *Chim. OGGI-Chem. Today* **2014**, *32*, 19–21.
15. Abadie, M.-A.; Trivelli, X.; Medina, F.; Capet, F.; Roussel, P.; Agbossou-Niedercorn, F.; Michon, C. Asymmetric Intramolecular Hydroamination of Alkenes in Mild and Wet Conditions—Structure and Reactivity of Cationic Binuclear Gold(I) Catalysts. *ChemCatChem* **2014**, *6*, 2235–2239. [CrossRef]
16. Abadie, M.-A.; Trivelli, X.; Medina, F.; Duhal, N.; Kouach, M.; Linden, B.; Vandewalle, M.; Capet, F.; Roussel, P.; Del Rosal, I.; et al. Gold(I)-Catalysed Asymmetric Hydroamination of Alkenes: A Silver- and Solvent-Dependent Enantiodivergent Reaction. *Chem. Eur. J.* **2017**, *23*, 10777–10788. [CrossRef] [PubMed]
17. Michon, C.; Medina, F.; Capet, F.; Roussel, P.; Agbossou-Niedercorn, F. Inter- and Intramolecular Hydroamination of Unactivated Alkenes Catalysed by a Combination of Copper and Silver Salts: The Unveiling of a Brønsted Acid Catalysis. *Adv. Synth. Catal.* **2010**, *352*, 3293–3305. [CrossRef]
18. Medina, F.; Michon, C.; Agbossou-Niedercorn, F. Intermolecular Mono- and Dihydroamination of Activated Alkenes Using a Recoverable Gold Catalyst. *Eur. J. Org. Chem.* **2012**, *2012*, 6218–6227. [CrossRef]
19. Michon, C.; Medina, F.; Abadie, M.-A.; Agbossou-Niedercorn, F. Asymmetric Intramolecular Hydroamination of Allenes using Mononuclear Gold Catalysts. *Organometallics* **2013**, *32*, 5589–5600. [CrossRef]
20. Michon, C.; Gilbert, J.; Trivelli, X.; Nahra, F.; Cazin, C.S.J.; Agbossou-Niedercorn, F.; Nolan, S.P. Gold(I) catalysed regio- and stereoselective intermolecular hydroamination of internal alkynes: Towards functionalised azoles. *Org. Biomol. Chem.* **2019**, *17*, 3805–3811. [CrossRef]
21. Bartók, M. Unexpected inversions in asymmetric reactions: Reactions with chiral metal complexes, chiral organocatalysts, and heterogeneous chiral catalysts. *Chem. Rev.* **2010**, *110*, 1663–1705. [CrossRef] [PubMed]
22. Escorihuela, J.; Burguete, M.I.; Luis, S.V. New advances in dual stereocontrol for asymmetric reactions. *Chem. Soc. Rev.* **2013**, *42*, 5595–5617. [CrossRef]
23. Beletskaya, I.P.; Nájera, C.; Yus, M. Stereodivergent Catalysis. *Chem. Rev.* **2018**, *118*, 5080–5200. [CrossRef] [PubMed]
24. Cao, W.; Feng, X.; Liu, X. Reversal of enantioselectivity in chiral metal complex-catalyzed asymmetric reactions. *Org. Biomol. Chem.* **2019**, *17*, 6538–6550. [CrossRef] [PubMed]
25. Saito, R.; Naruse, S.; Takano, K.; Fukuda, K.; Katoh, A.; Inoue, Y. Unusual Temperature Dependence of Enantioselectivity in Asymmetric Reductions by Chiral NADH Models. *Org. Lett.* **2006**, *8*, 2067–2070. [CrossRef]
26. Chan, V.S.; Chiu, M.; Bergman, R.G.; Toste, F.D. Development of Ruthenium Catalysts for the Enantioselective Synthesis of P-Stereogenic Phosphines via Nucleophilic Phosphido Intermediates. *J. Am. Chem. Soc.* **2009**, *131*, 6021–6032. [CrossRef]
27. Sohtome, Y.; Tanaka, S.; Takada, K.; Yamaguchi, T.; Nagasawa, K. Solvent-dependent enantiodivergent Mannich-type reaction: Utilizing a conformationally flexible guanidine/bisthiourea organocatalyst. *Angew. Chem. Int. Ed.* **2010**, *49*, 9254–9257. [CrossRef]
28. Chiarucci, M.; Mocci, R.; Syntrivanis, L.-D.; Cera, G.; Mazzanti, A.; Bandini, M. Merging synthesis and enantioselective functionalization of indoles by a gold-catalyzed asymmetric cascade reaction. *Angew. Chem. Int. Ed.* **2013**, *52*, 10850–10853. [CrossRef]
29. Davies, P.W.; Martin, N. Counterion Effects in a Gold-Catalyzed Synthesis of Pyrroles from Alkynyl Aziridines. *Org. Lett.* **2009**, *11*, 2293–2296. [CrossRef]

30. Fang, W.; Presset, M.; Guérinot, A.; Bour, C.; Bezzenine-Lafollée, S.; Gandon, V. Cationic gold(I)-catalyzed enantioselective hydroalkylation of unactivated alkenes: Influence of the chloride scavenger on the stereoselectivity. *Org. Chem. Front.* **2014**, *1*, 608–613. [CrossRef]
31. Jia, M.; Bandini, M. Counterion Effects in Homogeneous Gold Catalysis. *ACS Catal.* **2015**, *5*, 1638–1652. [CrossRef]
32. Jaroschik, F.; Simonneau, A.; Lemière, G.; Cariou, K.; Agenet, N.; Amouri, H.; Aubert, C.; Goddard, J.-P.; Lesage, D.; Malacria, M.; et al. Assessing Ligand and Counterion Effects in the Noble Metal Catalyzed Cycloisomerization Reactions of 1,6-Allenynes: A Combined Experimental and Theoretical Approach. *ACS Catal.* **2016**, *6*, 5146–5160. [CrossRef]
33. Ilg, M.K.; Wolf, L.M.; Mantilli, L.; Farès, C.; Thiel, W.; Fürstner, A. A Striking Case of Enantioinversion in Gold Catalysis and Its Probable Origins. *Chem. Eur. J.* **2015**, *21*, 12279–12284. [CrossRef] [PubMed]
34. Macchioni, A. Ion Pairing in Transition-Metal Organometallic Chemistry. *Chem. Rev.* **2005**, *105*, 2039–2074. [CrossRef] [PubMed]
35. Pregosin, P.S. NMR spectroscopy and ion pairing: Measuring and understanding how ions interact. *Pure Appl. Chem.* **2009**, *81*, 615–633. [CrossRef]
36. Kanno, O.; Kuriyama, W.; Wang, J.Z.; Toste, D.F. Regio- and enantioselective hydroamination of dienes by gold(I)/menthol cooperative catalysis. *Angew. Chem. Int. Ed.* **2011**, *50*, 9919–9922. [CrossRef]
37. Lutz, F.; Igarashi, T.; Kinoshita, T.; Asahina, M.; Tsukiyama, K.; Kawasaki, T.; Soai, K. Mechanistic Insights in the Reversal of Enantioselectivity of Chiral Catalysts by Achiral Catalysts in Asymmetric Autocatalysis. *J. Am. Chem. Soc.* **2008**, *130*, 2956–2958. [CrossRef]
38. Nojiri, A.; Kumagai, N.; Shibasaki, M. Linking structural dynamics and functional diversity in asymmetric catalysis. *J. Am. Chem. Soc.* **2009**, *131*, 3779–3784. [CrossRef]
39. Wang, Z.; Yang, Z.; Chen, D.; Liu, X.; Lin, L.; Feng, X. Highly Enantioselective Michael Addition of Pyrazolin-5-ones Catalyzed by Chiral Metal/N,N′-Dioxide Complexes: Metal-Directed Switch in Enantioselectivity. *Angew. Chem. Int. Ed.* **2011**, *50*, 4928–4932. [CrossRef]
40. Lu, G.; Yoshino, T.; Morimoto, H.; Matsunaga, S.; Shibasaki, M. Stereodivergent direct catalytic asymmetric Mannich-type reactions of α-isothiocyanato ester with ketimines. *Angew. Chem. Int. Ed.* **2011**, *50*, 4382–4385. [CrossRef]
41. Noble-Terán, M.E.; Buhse, T.; Cruz, J.M.; Coudret, C.; Micheau, J.C. Nonlinear Effects in Asymmetric Synthesis: A Practical Tool for the Discrimination between Monomer and Dimer Catalysis. *ChemCatChem* **2016**, *8*, 1836–1845. [CrossRef]
42. Satyanarayana, T.; Abraham, S.; Kagan, H.B. Nonlinear effects in asymmetric catalysis. *Angew. Chem. Int. Ed.* **2009**, *48*, 456–494. [CrossRef]
43. Hu, J.-Y.; Zhang, J.; Wang, G.-X.; Sun, H.-L.; Zhang, J.-L. Constructing a Catalytic Cycle for C-F to C-X (X = O, S, N) Bond Transformation Based on Gold-Mediated Ligand Nucleophilic Attack. *Inorg. Chem.* **2016**, *55*, 2274–2283. [CrossRef] [PubMed]
44. Garcia-Simon, C.; Garcia-Borras, M.; Gomez, L.; Garcia-Bosch, I.; Osuna, S.; Swart, M.; Luis, J.P.; Rovira, C.; Almeida, M.; Imaz, I.; et al. Self-Assembled Tetragonal Prismatic Molecular Cage Highly Selective for Anionic π Guests. *Chem. Eur. J.* **2013**, *19*, 1445–1456. [CrossRef]
45. Zhou, Q.; Li, Y. 1,3-Cationic Alkylidene Migration of Nonclassical Carbocation: A Density Functional Theory Study on Gold(I)-Catalyzed Cycloisomerization of 1,5-Enynes Containing Cyclopropene Moiety. *J. Am. Chem. Soc.* **2014**, *136*, 1505–1513. [CrossRef]
46. Herrero-Gómez, E.; Nieto-Oberhuber, C.; López, S.; Benet-Buchholz, J.; Echavarren, A.M. Cationic η^1/η^2-gold(I) complexes of simple arenes. *Angew. Chem. Int. Ed.* **2006**, *45*, 5455–5459. [CrossRef]
47. Chifotides, H.T.; Dunbar, K.R. Anion-π Interactions in Supramolecular Architectures. *Acc. Chem. Res.* **2013**, *46*, 894–906. [CrossRef]
48. Dougherty, D.A. The Cation-π Interaction. *Acc. Chem. Res.* **2013**, *46*, 885–893. [CrossRef]
49. Mahadevi, A.S.; Sastry, G.N. Cation-π interaction: Its role and relevance in chemistry, biology, and material science. *Chem. Rev.* **2013**, *113*, 2100–2138. [CrossRef]
50. Weber, D.; Gagné, M.R. Dinuclear gold-silver resting states may explain silver effects in gold(I)-catalysis. *Org. Lett.* **2009**, *11*, 4962–4965. [CrossRef]
51. Wang, D.; Cai, R.; Sharma, S.; Jirak, J.; Thummanapelli, S.K.; Akhmedov, N.G.; Zhang, H.; Liu, X.; Petersen, J.L.; Shi, X. Silver effect in gold(I) catalysis: An overlooked important factor. *J. Am. Chem. Soc.* **2012**, *134*, 9012–9019. [CrossRef]
52. Zhu, Y.; Day, C.S.; Zhang, L.; Hauser, K.J.; Jones, A.C. A Unique Au-Ag-Au Triangular Motif in a Trimetallic Halonium Dication: Silver Incorporation in a Gold(I) Catalyst. *Chem. Eur. J.* **2013**, *19*, 12264–12271. [CrossRef] [PubMed]
53. Homs, A.; Escofet, I.; Echavarren, A.M. On the silver effect and the formation of chloride-bridged digold complexes. *Org. Lett.* **2013**, *15*, 5782–5785. [CrossRef] [PubMed]
54. Su, Y.; Lu, M.; Dong, B.; Chen, H.; Shi, X. Silver-Catalyzed Alkyne Activation: The Surprising Ligand Effect. *Adv. Synth. Catal.* **2014**, *356*, 692–696. [CrossRef]
55. Fang, W.; Presset, M.; Guérinot, A.; Bour, C.; Bezzenine-Lafollée, S.; Gandon, V. Silver-Free Two-Component Approach in Gold Catalysis: Activation of [LAuCl] Complexes with Derivatives of Copper, Zinc, Indium, Bismuth, and Other Lewis Acids. *Chem. Eur. J.* **2014**, *20*, 5439–5446. [CrossRef] [PubMed]
56. Zhdanko, A.; Maier, M.E. Explanation of Silver Effects in Gold(I)-Catalyzed Hydroalkoxylation of Alkynes. *ACS Catal.* **2015**, *5*, 5994–6004. [CrossRef]
57. Xu, G.; Liu, K.; Dai, Z.; Sun, J. Gold/silver-catalyzed controllable regioselective vinylcarbene insertion into O-H bonds. *Org. Biomol. Chem.* **2017**, *15*, 2345–2348. [CrossRef]

58. Veguillas, M.; Rosair, G.M.; Bebbington, M.W.P.; Lee, A.-L. Silver Effect in Regiodivergent Gold-Catalyzed Hydroaminations. *ACS Catal.* **2019**, *9*, 2552–2557. [CrossRef]
59. Franchino, A.; Montesinos-Magraner, M.; Echavarren, A.M. Silver-Free Catalysis with Gold(I) Chloride Complexes. *Bull. Chem. Soc. Jpn.* **2021**, *94*, 1099–1117. [CrossRef]
60. Kim, U.B.; Jung, D.J.; Jeon, H.J.; Rathwell, K.; Lee, S. Synergistic Dual Transition Metal Catalysis. *Chem. Rev.* **2020**, *120*, 13382–13433. [CrossRef]
61. Bayler, A.; Bauer, A.; Schmidbaur, H. Synthesis and Structure of Binuclear Single-Bridged Bis[(phosphane)gold(I)]halogenonium Complexes. *Chem. Ber.* **1997**, *130*, 115–118. [CrossRef]
62. Hamel, A.; Mitzel, N.W.; Schmidbaur, H. Metallophilicity: The dimerization of bis[(triphenylphosphine)gold(I)]chloronium cations. *J. Am. Chem. Soc.* **2001**, *123*, 5106–5107. [CrossRef] [PubMed]
63. Schmidbaur, H.; Hamel, A.; Mitzel, N.W.; Schier, A.; Nogai, S. Cluster self-assembly of di[gold(I)]halonium cations. *Proc. Natl. Acad. Sci. USA* **2002**, *99*, 4916–4921. [CrossRef] [PubMed]
64. Zhang, K.; Prabhavathy, J.; Yip, J.H.K.; Koh, L.L.; Tan, G.K.; Vittal, J.J. First Examples of AuI-X-AgI Halonium Cations (X = Cl and Br). *J. Am. Chem. Soc.* **2003**, *125*, 8452–8453. [CrossRef] [PubMed]
65. Weber, S.G.; Rominger, F.; Straub, B.F. Isolated Silver Intermediate of Gold Precatalyst Activation. *Eur. J. Inorg. Chem.* **2012**, *2012*, 2863–2867. [CrossRef]
66. Simonneau, A.; Jaroschik, F.; Lesage, D.; Karanik, M.; Guillot, R.; Malacria, M.; Tabet, J.-C.; Goddard, J.-P.; Fensterbank, L.; Gandon, V.; et al. Tracking gold acetylides in gold(I)-catalyzed cycloisomerization reactions of enynes. *Chem. Sci.* **2011**, *2*, 2417–2422. [CrossRef]
67. Zhdanko, A.; Maier, M.E. Synthesis of gem-Diaurated Species from Alkynols. *Chem. Eur. J.* **2013**, *19*, 3932–3942. [CrossRef] [PubMed]
68. Schulz, J.; Shcherbachenko, E.; Roithová, J. Investigation of Geminally Diaurated Arene Complexes in the Gas Phase. *Organometallics* **2015**, *34*, 3979–3987. [CrossRef]
69. Linden, H.B. Liquid injection field desorption ionization: A new tool for soft ionization of samples including air sensitive catalysts and non-polar hydrocarbons. *Eur. J. Mass Spectrom.* **2004**, *10*, 459–468. [CrossRef]
70. Gross, J.H.; Nieth, N.; Linden, H.B.; Blumbach, U.; Richter, F.J.; Tauchert, M.E.; Tompers, R.; Hofmann, P. Liquid injection field desorption/ionization of reactive transition metal complexes. *Anal. Bioanal. Chem.* **2006**, *386*, 52–58. [CrossRef] [PubMed]
71. LaLonde, R.L.; Brenzovich, W.E.; Benitez, D.; Tkatchouk, E.; Kelley, K.; Goddard, W.A., III; Toste, F.D. Alkylgold complexes by the intramolecular aminoauration of unactivated alkenes. *Chem. Sci.* **2010**, *1*, 226–233. [CrossRef] [PubMed]
72. Gaggioli, C.A.; Ciancaleoni, G.; Zuccaccia, D.; Bistoni, G.; Belpassi, L.; Tarantelli, F.; Belanzoni, P. Strong Electron-Donating Ligands Accelerate the Protodeauration Step in Gold(I)-Catalyzed Reactions: A Quantitative Understanding of the Ligand Effect. *Organometallics* **2016**, *35*, 2275–2285. [CrossRef]
73. Couce-Rios, A.; Lledós, A.; Fernández, I.; Ujaque, G. Origin of the Anti-Markovnikov Hydroamination of Alkenes Catalyzed by L-Au(I) Complexes: Coordination Mode Determines Regioselectivity. *ACS Catal.* **2019**, *9*, 848–858. [CrossRef]
74. Gubler, J.; Radić, M.; Stöferle, Y.; Chen, P. 2-Aminoalkylgold Complexes: The Putative Intermediate in Au-Catalyzed Hydroamination of Alkenes Does Not Protodemetalate. *Chem. Eur. J.* **2022**, *28*, e202200332. [CrossRef] [PubMed]
75. Liu, X.-Y.; Guo, Z.; Dong, S.S.; Li, X.-H.; Che, C.-M. Highly Efficient and Diastereoselective Gold(I)-Catalyzed Synthesis of Tertiary Amines from Secondary Amines and Alkynes: Substrate Scope and Mechanistic Insights. *Chem. Eur. J.* **2011**, *17*, 12932–12945. [CrossRef]
76. Katari, M.; Rao, M.N.; Rajaraman, G.; Ghosh, P. Computational Insight into a Gold(I) N-Heterocyclic Carbene Mediated Alkyne Hydroamination Reaction. *Inorg. Chem.* **2012**, *51*, 5593–5604. [CrossRef]
77. Alvarado, E.; Badaj, A.C.; Larocque, T.G.; Lavoie, G.G. N-Heterocyclic Carbenes and Imidazole-2-thiones as Ligands for the Gold(I)-Catalysed Hydroamination of Phenylacetylene. *Chem. Eur. J.* **2012**, *18*, 12112–12121. [CrossRef]
78. Brooner, R.E.M.; Windenhoefer, R.A. Cationic, two-coordinate gold π complexes. *Angew. Chem. Int. Ed.* **2013**, *52*, 11714–11724. [CrossRef]
79. Kovács, G.; Ujaque, G.; Lledós, A. The Reaction Mechanism of the Hydroamination of Alkenes Catalyzed by Gold(I)-Phosphine: The Role of the Counterion and the N-Nucleophile Substituents in the Proton-Transfer Step. *J. Am. Chem. Soc.* **2008**, *130*, 853–864. [CrossRef]
80. Appelhans, L.N.; Zuccaccia, D.; Kovacevic, A.; Chianese, A.R.; Miecznikowski, J.R.; Macchioni, A.; Clot, E.; Eisenstein, O.; Crabtree, R.H. An anion-dependent switch in selectivity results from a change of C-H activation mechanism in the reaction of an imidazolium salt with $IrH_5(PPh_3)_2$. *J. Am. Chem. Soc.* **2005**, *127*, 16299–16311. [CrossRef]
81. Davies, D.L.; Donald, S.M.A.; Macgregor, S.A. Computational study of the mechanism of cyclometalation by palladium acetate. *J. Am. Chem. Soc.* **2005**, *127*, 13754–13755. [CrossRef] [PubMed]
82. García-Cuadrado, D.; Braga, A.A.C.; Maseras, F.; Echavarren, A.M. Proton abstraction mechanism for the palladium-catalyzed intramolecular arylation. *J. Am. Chem. Soc.* **2006**, *128*, 1066–1067. [CrossRef] [PubMed]
83. Basallote, M.G.; Besora, M.; Castillo, C.E.; Fernández-Trujillo, M.J.; Lledós, A.; Maseras, F.; Máñez, M.A. Crucial role of anions on the deprotonation of the cationic dihydrogen complex trans-$[FeH(\eta^2\text{-}H_2)(dppe)_2]^+$. *J. Am. Chem. Soc.* **2007**, *129*, 6608–6618. [CrossRef] [PubMed]

84. Mishra, H.; Enami, S.; Nielsen, R.J.; Hoffmann, M.R.; Goddard, W.A., III; Colussi, A.J. Anions dramatically enhance proton transfer through aqueous interfaces. *Proc. Natl. Acad. Sci. USA* **2012**, *109*, 10228–10232. [CrossRef] [PubMed]
85. Munz, D.; Webster-Gardiner, M.; Fu, R.; Strassner, T.; Goddard, W.A., III; Gunnoe, T.B. Proton or Metal? The H/D Exchange of Arenes in Acidic Solvents. *ACS Catal.* **2015**, *5*, 769–775. [CrossRef]
86. Zhang, J.; Shen, W.; Li, L.; Li, M. Gold(I)-Catalyzed Cycloaddition of 1-(1-Alkynyl)cyclopropyl Ketones with Nucleophiles To Yield Substituted Furans: A DFT Study. *Organometallics* **2009**, *28*, 3129–3139. [CrossRef]
87. Krauter, C.M.; Hashmi, A.S.K.; Pernpointner, M. A New Insight into Gold(I)-Catalyzed Hydration of Alkynes: Proton Transfer. *ChemCatChem* **2010**, *2*, 1226–1230. [CrossRef]
88. Cavallo, G.; Metrangolo, P.; Milani, R.; Pilati, T.; Priimagi, A.; Resnati, G.; Terraneo, G. The Halogen Bond. *Chem. Rev.* **2016**, *116*, 2478–2601. [CrossRef]
89. Robertson, C.C.; Wright, J.S.; Carrington, E.J.; Perutz, R.N.; Hunter, C.A.; Brammer, L. Hydrogen bonding vs. halogen bonding: The solvent decides. *Chem. Sci.* **2017**, *8*, 5392–5398. [CrossRef]
90. Sutar, R.L.; Huber, S.M. Catalysis of Organic Reactions through Halogen Bonding. *ACS Catal.* **2019**, *9*, 9622–9639. [CrossRef]
91. Perchloric Acid as Well as All Organic and Organometallic Perchlorate Salts Are Often Explosive and Are Thus Highly Dangerous. Available online: http://ehs.berkeley.edu/lessons-learned/lesson-learned-chemical-explosion-causes-eye-injury (accessed on 7 November 2022).
92. TURBOMOLE V7.1 2016, a Development of University of Karlsruhe and Forschungszentrum Karlsruhe GmbH, 1989–2007, TURBOMOLE GmbH, Since 2007. Available online: http://www.turbomole.com (accessed on 7 November 2022).
93. Perdew, J.P.; Burke, K.; Ernzerhof, M. Generalized Gradient Approximation Made Simple. *Phys. Rev. Lett.* **1996**, *77*, 3865–3869. [CrossRef] [PubMed]
94. Schäfer, A.; Huber, C.; Ahlrichs, R. Fully optimized contracted Gaussian basis sets of triple zeta valence quality for atoms Li to Kr. *J. Chem. Phys.* **1994**, *100*, 5829–5835. [CrossRef]
95. Weigend, F.; Ahlrichs, R. Balanced basis sets of split valence, triple zeta valence and quadruple zeta valence quality for H to Rn: Design and assessment of accuracy. *Phys. Chem. Chem. Phys.* **2005**, *7*, 3297–3305. [CrossRef] [PubMed]
96. Weigend, F. Accurate Coulomb-fitting basis sets for H to Rn. *Phys. Chem. Chem. Phys.* **2006**, *8*, 1057–1065. [CrossRef]
97. Adamo, C.; Barone, V. Toward reliable density functional methods without adjustable parameters: The PBE0 model. *J. Chem. Phys.* **1999**, *110*, 6158–6169. [CrossRef]
98. Eichkorn, K.; Treutler, O.; Öhm, H.; Häser, M.; Ahlrichs, R. Auxiliary basis sets to approximate Coulomb potentials. *Chem. Phys. Lett.* **1995**, *240*, 283–290. [CrossRef]
99. Sierka, M.; Hogekamp, A.; Ahlrichs, R. Fast evaluation of the Coulomb potential for electron densities using multipole accelerated resolution of identity approximation. *J. Chem. Phys.* **2003**, *118*, 9136–9148. [CrossRef]
100. Klamt, A.; Schüürmann, G. COSMO: A new approach to dielectric screening in solvents with explicit expressions for the screening energy and its gradient. *J. Chem. Soc. Perkin Trans. 2* **1993**, 799–805. [CrossRef]
101. Grimme, S.; Antony, J.; Ehrlich, S.; Krieg, H. A consistent and accurate ab initio parametrization of density functional dispersion correction (DFT-D) for the 94 elements H-Pu. *J. Chem. Phys.* **2010**, *132*, 154104. [CrossRef]
102. Lu, T.; Chen, F. Multiwfn: A multifunctional wavefunction analyzer. *J. Comput. Chem.* **2012**, *33*, 580–592. [CrossRef]
103. Humphrey, W.; Dalke, A.; Schulten, K. VMD: Visual molecular dynamics. *J. Mol. Graph.* **1996**, *14*, 33–38. [CrossRef]
104. Kamalakannan, S.; Prakash, M.; Chambaud, G.; Hochlaf, M. Adsorption of Hydro-phobic and Hydrophilic Ionic Liquids at the Au(111) Surface. *ACS Omega* **2018**, *3*, 18039–18051. [CrossRef] [PubMed]
105. Liu, D.-J.; Lee, J.; Windus, T.L.; Thiel, P.A.; Evans, J.W. Sulfur-enhanced dynamics of coinage metal(111) surfaces: Step edges versus terraces as locations for metal-sulfur complex formation. *Surf. Sci.* **2018**, *676*, 2–8. [CrossRef]
106. Pounder, A.; Tam, W.; Chen, L.D. The Mechanism and Origin of Enantioselectivity in the RhodiumCatalyzed Asymmetric Ring-Opening Reactions of Oxabicyclic Alkenes with Organoboronic Acids: A DFT Investigation. *Organometallics* **2021**, *40*, 1588–1597. [CrossRef]